ChemComm

XPS studies of surface of metal catalyst nanoparticles in a flowing liquid

Journal:	*ChemComm*
Manuscript ID	CC-COM-04-2018-003497.R1
Article Type:	Communication

XPS studies of surface of metal catalyst nanoparticles in a flowing liquid

Luan Nguyen,[a] Paul (Pengcheng) Tao,[a] Huimin Liu, [a,b] Mohamed Al-Hada,[c] Matteo Amati, [c] Hikmet Sezen, [c] Yu Tang,[a] Luca Gregoratti ,[c]* and Franklin (Feng) Tao [a]*

[a]Department of Chemical and Petroleum Engineering, University of Kansas, Lawrence, KS 66045, USA
[b] School of Chemical and Biomolecular Engineering, The University of Sydney, Sydney, New South Wales 2006, Australia
[c]Elettra - Sincrotrone Trieste ScPA, Trieste 34012, Italy

Abstract: Studying surface of catalyst nanoparticles in a flowing liquid under its working condition is significant to predict its catalytic performance and understand the underlying reaction mechanism. X-ray photoelectron spectroscopy (XPS) is one of the main techniques for examining surface of a catalyst. However, study of catalyst nanoparticles in a flowing liquid via XPS is hindered by (1) the short inelastic mean free path of photoelectrons in liquid and (2) the high vapour pressure of liquid containing catalyst nanoparticles. Here we report the design of a reaction system of a Si_3N_4 cell with window cover electron-transmissible membrane which overcame the above limitations. By using Ag nanoparticles as a catalyst dispersed in solvent (a mixture of tripropylene glycol methyl ether and phenol), the capability of examining surface of catalyst nanoparticles in a flowing liquid was demonstrated by the successful observation of Ag 3d photoemission feature when the liquid containing Ag nanoparticles was flowing through this reaction system. This work developed a new method of studying surface of catalyst nanoparticles functioning in a flowing liquid for mechanistically understanding heterogeneous catalysis performed at solid/liquid interface.

Unravelling surface of a catalyst during catalysis, where a catalytic reaction occurs [1-3], is crucial in understanding its reaction mechanism and rationally designing a better catalyst. The surface chemistry of a catalyst, including elemental composition, and chemical and electronic states of the elements, could be quantitatively analyzed via X-ray photoelectron spectroscopy (XPS), an important technique known for high surface sensitivity and specificity [4, 5]. In many cases, the surface chemistry of a catalyst is characterized via ex situ XPS with the catalyst being placed in ultrahigh vacuum (UHV, $<1\times10^{-8}$ Torr) of analysis chamber of XPS; the results obtained via ex-situ XPS characterization could not guarantee to truly reflect the surface of a catalyst under its working condition because the high density of molecules of reactants of liquid phase could potentially modify or restructure catalyst surface [6]. A large portion of industrial catalytic reactions are performed on surface of catalyst nanoparticles dispersing in flowing liquids containing reactants, products, solvents and catalyst nanoparticles. [7, 8] Scientists have realized the significance of surface chemistry of catalyst nanoparticles in a flowing liquid in fundamental understanding of heterogeneous catalysis performed in liquid at a molecular level. Therefore, it is of great significance to develop method using XPS technique to investigate the surface of a catalyst.

Preparation of a reaction system. A large portion of catalytic reactions of chemical industries are performed on surface of catalyst nanoparticles dispersed in liquids. During these catalytic reactions, catalyst nanoparticles are stirred; alternatively, liquid phase of reactants, products and solvents flows through a catalyst. To simulate surface of a catalyst nanoparticles in liquid under these catalytic conditions, here we designed a reaction system with one electron-transparent graphene membrane with thickness of about 6-7 Å to separate the liquid from the UHV environment of XPS analysis chamber as well as with an inlet and an outlet for flowing the liquid containing solvent and reactant and catalyst nanoparticles (Figure S1). This reaction system enables observation of surface of catalyst nanoparticles dispersed in the flowing liquid via XPS. In this study, Ag nanoparticles (catalyst) dispersed a mixture of tripropylene glycol methyl ether and phenol is selected as a probe system and the surface of Ag nanoparticles was characterized when the liquid was flowing through the designed graphene membrane covered on Si_3N_4 window. Here Ag nanoparticle was chosen due to its relevance as a catalyst in many heterogeneous catalytic processes such as transformation of organics and synthesis of fine chemicals [9], fuel cells [10], photocatalytic devices [11], and catalytic converters [12].in flowing liquid during catalysis.

Regarding the study of surface of catalyst nanoparticles in liquid, approaches have been developed for investigation of a liquid/solid interface between catalyst nanoparticles and molecules of liquid via XPS, including dip-and-pull method [13, 14], liquid microjet method [15-18] and method using a cell [19-21]. As for the dip-and-pull method, the liquid/solid interface is formed by dipping a flat substrate with anchored catalyst nanoparticles to liquid and then pulling the sample out from the liquid. A thin layer of liquid remains on the sample surface after dipping and pulling steps, forming a solid-liquid interface. The specific solid surface covered with enough thin liquid (< 10 nm) can be analyzed by XPS; in this method a differentially pumped electron energy analyzer is used since vapor pressure of liquid typically in a few to a few tens of torr pressure range [13, 14] is much higher the working pressure ($<10^{-6}$ Torr) of a standard energy analyzer. In addition, at an elevated temperature such as 80°C, most liquid thin film above catalyst nanoparticles could completely vaporize immediately, which limits a potential application of this method to a relatively high temperature. In addition, the liquid in dip-and-pull method can study solid surface below a liquid thin film at a static state instead of a moving or flowing state since the X-ray beam has to face to the exact location where its liquid is thin enough (<10 nm). This limit excludes its application to studies of liquid/solid interface in a flowing system.

In liquid microjet method, the liquid containing catalyst nanoparticles forms a microjet flow via a nozzle and enters XPS analysis chamber, where it receives X-ray irradiation and generates photoelectrons [15, 16, 18, 22]. Different from dip-and-pull method, liquid microjet method allows the analysis of liquid/solid interface in a flowing system. Similar to the dip-and-pull method, a differentially pumped energy analyzer is compulsory since the pressure around the microjet flow is in the range of 10^{-4}~10^{-2} Torr, much higher than the typical working vacuum of a typical UHV XPS electron energy analyzer ($<1\times10^{-6}$ Torr). In addition, it is reluctant to analyze catalyst nanoparticles with relatively larger sizes or dispersed with relatively high concentration, as catalyst particles of larger sizes or high concentration in a liquid might clog the jet nozzle. To our knowledge, XPS study above room temperature using liquid microjet method has not been realized due to technical challenge in heating a flowing micro bead-like droplets.

Cell sealed with a membrane window is an approach used for isolating liquid from high vacuum while the membrane allows for transmission of electron beam or/and photon flux. Si_3N_4 membrane-based cell containing nanoparticles was used for studying growth of metal nanoparticle by Zheng et al and other group.[20] Graphene membrane cell has been used for a similar

purpose. It breaks through the limitations encountered by the liquid microjet method. In graphene window method, the liquid containing catalyst nanoparticles is completely isolated from the UHV environment of XPS analysis chamber, which makes a standard energy analyzer sufficient for XPS studies. By using a liquid cell, O 1s of liquid H_2O was measured. [21, 23-25] Recent study of Velasco et al. [25] reported XPS investigations of cobalt atoms at the interface between graphene window and cobalt oxide thin film deposited on the window, in which a cell window containing multiple graphene membrane openings was used in order to collect enough photoelectron signals. To the best of our knowledge, study of surface of nanoparticles *dispersed* in a flowing liquid has not been reported.

As the main target of this study is to investigate surface of catalyst nanoparticles dispersed in a flowing liquid, it is crucial to design a reactor in which the liquid containing solvent, reactants and catalyst nanoparticles can flow. Here, a flowing liquid reactor with an inlet and an outlet for the flow of the liquid shown in Figures 1a, 1b and 1c was designed. During an experiment, the reactor for XPS studies was mounted on a sample stage (Figure 1d). A syringe pump at the inlet was used to inject the liquid containing catalyst nanoparticles (Figure 1a). The continuous injection made liquid flow through the Si3N4 window covered with graphene membrane and exit through the outlet port of the reactor. The flow direction and the location of the graphene membrane cell are shown in Figure 1c. This specially designed configuration of the liquid cell in Figure 1c made sure the injected liquid reach surface of graphene and thus formed a graphene-liquid interface. Formation of a graphene-liquid interface is significant. This is because surface of catalyst nanoparticles in liquid could be studied only when there is a graphene-liquid interface. Figure 1d is the well prepared main part of the liquid reaction system. The inlet and outlet tubing were connected with UHV chamber through two 2.85" conflat flange with feedthrough as shown in Figure S1.

Preparation of Si_3N_4 membrane cell with a window. The flow cell is the most important part of the designed reaction system. For the liquid/solid interface studies using a flow cell covered with a graphene window, only the photoelectrons generated from the volume within the sampling depth can be collected. Considering a generated photoelectron with kinetic energy <1000 eV, its sampling depths in solvent and in Si_3N_4 are calculated to be < 10.3 nm and < 7.2 nm (three times of their inelastic mean free paths, IMFP, which is derived from TPP-2M equation [26]), respectively. Then, the photoelectrons with kinetic energy <1000 eV could not penetrate Si_3N_4 membrane to be collected by energy analyzer, because its sampling depth in Si_3N_4 (< 7.2 nm) is much smaller than the thickness of Si_3N_4 membrane (30 nm). Thus, here the center of Si_3N_4 membrane was replaced with a graphene membrane, by which the photoelectrons generated from the surface of catalyst nanoparticles within 10.3 nm deep in the liquid could easily travel through the graphene membrane and reach to XPS energy analyzer, as a two-layer graphene is almost photoelectron transparent. As the collectable photoelectron intensity is exponentially decay along the increase of depth, it is still a technique with high surface sensitivity. As solvent molecules between metal NPs and graphene decays photoelectron intensity largely, only surface layers of Ag NPs contribute to signal of XPS peak in this case.

The graphene window was fabricated via the following three steps. A through pore was made on Si_3N_4 membrane via Ga ion-beam milling setup in a scanning electron microscope; Cr thin film with a thickness of 50 nm and an Au thin film with a thickness of 100 nm were then consecutively deposited on both sides of Si_3N_4 window with the aim to increase the adhesion between the Si_3N_4 window and graphene layers or prevent sample surface charging during XPS experiments; the thorough hole on Si_3N_4 was covered by a two-layer graphene membrane by transferring graphene layers of graphene/Cu foil onto Au/Cr/Si_3N_4/Cr/Au. The detailed procedures are illustrated in Figure S2 and descried in its note in the supporting information. The SEM image of the graphene window in Figure 2d suggests that the thorough pore on Si_3N_4 membrane was successfully covered by a two-layer graphene membrane and thus a graphene window was prepared.

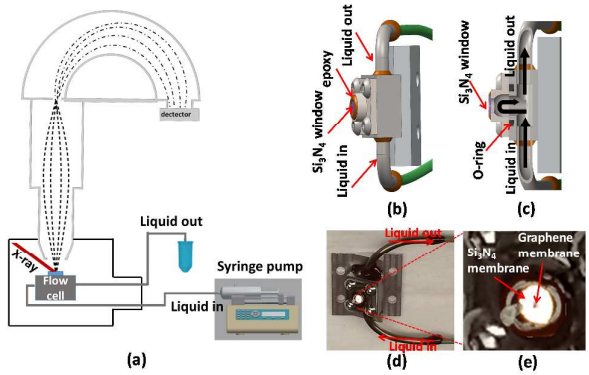

Figure 1. Reactor system designed for studies of surface of catalyst NPs in flowing liquid. (a) Schematic of the whole system. (b) and (c) External and internal view of the Si_3N_4 cell; the brown ring shows the epoxy instead of O-ring; the epoxy was used to externally seal the two parts. (d) Photo of the reaction cell. (e) Enlargement of graphene membrane on Si_3N_4 membrane.

Metal nanoparticles dispersed in liquid remained in Si_3N_4 cell. To demonstrate the feasibility of studying surface of catalyst nanoparticles in a flowing liquid, a mixture of tripropylene glycol methyl ether and phenol with dispersed Ag nanoparticles was selected as a liquid and was injected into the designed reaction system (Figure 1a) at a flowrate of 0.5 mL·min^{-1}. Then, the inlet and outlet ports of the reaction system were sealed off temporarily to form a batch reactor (Figure 3a) for scanning electron microscope (SEM) analysis, which was used to check whether the graphene membrane cell with filled liquid was successfully prepared. In the SEM image in Figure 3a, obvious bright spots were observed in the dark circular region, attributable to Ag nanoparticles dispersed in the solvent below the graphene window. This observation verified the dispersion of Ag nanoparticles in the filled Si_3N_4 cell. Energy dispersive X-ray spectroscopy (EDS) of SEM was used to further analyze the elements below the graphene window of spot B (in-graphene window region) of the filled reaction cell and elements at spot A (off-graphene window area). Clearly, the peaks contributed from C, O, Si and Au at spot A, were detected in EDS (Figure 3d), originating from graphene covered Au/Cr/Si_3N_4/Cr/Au. Compared to EDS of spot A, there were no peaks of Si and Au in the EDS spectrum of spot B (Figure 3e) since the original material Au/Cr/Si_3N_4/Cr/Au was drilled out by ion beam and then covered with graphene membrane in the preparation (Figure S2). In addition, an additional peak at ~3.0 keV at spot B corresponding to Ag was clearly observed, confirming the existence of Ag nanoparticles in the Si_3N_4 cell (Figure 3e). Both SEM image (Figure

3c) and EDX spectrum analysis (Figure 3e) confirmed the successful preparation of a Si_3N_4 cell with window covered with graphene membrane in which the liquid containing Ag nanoparticles was well isolated from high vacuum environment.

As shown in Figure 3c, the bright spots appeared in graphene window region representing intensity of back-scattered electrons from Ag nanoparticles in solvent. Obviously, some of them are brighter than others. The brightness of these spots roughly reflect the location of the source of back-scattered electrons. The observation of bright spots of Ag nanoparticles with different contrasts suggests that there are substantial amount of Ag nanoparticles at deeper regions in the liquid although it is challenging to obtain quantitative information on the depth-distribution of Ag nanoparticles in solvent below a graphene membrane.

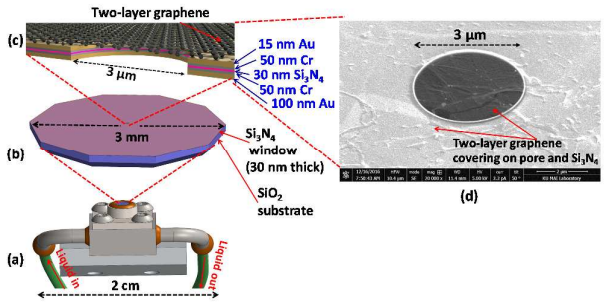

Figure 2. Structure of Si_3N_4 membrane cell with a window covered with a two-layer graphene membrane. (a) Reaction system of flowing liquid. (b) Si_3N_4 membrane grown on silicon wafer; in the middle of wafer, there is only Si_3N_4 membrane (30 nm thick). (c) Cross section view of pore of Si_3N_4 and the supported graphene membrane. (d) SEM image of two-layer graphene membrane covering the window of Si_3N_4 membrane.

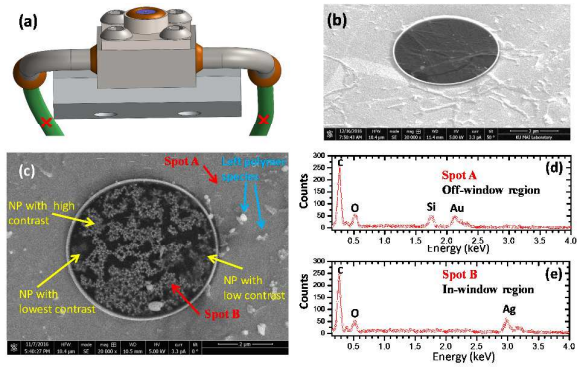

Figure 3. SEM studies of the reactor filled with solution of Ag NPs. (a) Drawing of the designed reaction system. (b) SEM image of window of Si_3N_4 membrane cell covered with a two-layer graphene membrane without solution of Ag NPs. (c) SEM image of Si_3N_4 cell covered with a two-layer graphene membrane filled with solution of Ag NPs (liquid didn't flow). (d) SEM-EDX spectrum at spot A (Si_3N_4 region in terms of the off- window region) of the Si_3N_4 cell. (e) SEM-EDX spectrum at spot B (in-window region) of the Si_3N_4 cell.

Examination of Si_3N_4 cell filled with ambient gas at 1 bar. The successfully designed flowing liquid reaction cell was employed to investigate the surface of Ag nanoparticles dispersed in a flowing liquid via XPS. The ESCA Microscopy beamline at Elettra-Sincrotrone Trieste ScPA, Italy was used to image the distribution of Ag nanoparticles. An X-ray beam of 1069 eV photon energy was used and the kinetic energy of the generated Ag $3d_{5/2}$ photoelectrons is about 701.6 eV. As IMFP of photoelectrons of 701.6 eV in Ag nanoparticles is ~11 Å [27] and Ag inter-planar distance is 2.36 Å (by taking Ag(111) as an example)[28], only the photoelectrons generated ~13.8 layers deep from surface could travel to the surface of Ag nanoparticles. Considered the fact that solvent molecules between Ag surface and graphene membrane attenuate the intensity of photoelectrons, the collected photoelectron intensity of Ag 3d by XPS analyzer are originated from surface/subsurface region of Ag nanoparticles.

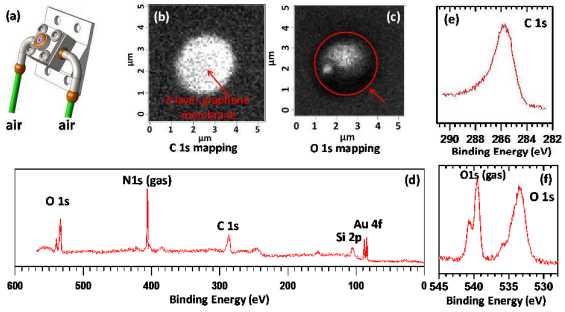

Figure 4. Blank experiment of a well prepared reaction system when the cell was open to ambient (1 bar of air). (a) Reactor filled with air. (b) Mapping of C1s photoelectron intensity. (c) Mapping of O 1s of O_2 in air. (d) XPS Survey of the graphene window region of Si_3N_4 membrane of the reactor. (e) C 1s peak of graphene membrane. (f) O 1s peaks of O_2 of air and oxygen-containing species left in graphene membrane during preparation.

Before studying the surface of Ag nanoparticles in a flowing liquid, XPS images of the graphene window region of an empty reaction cell filled with air were performed as a blank experiment. Mappings of intensities of C 1s photoelectrons generated from graphene membrane and O 1s photoelectrons released from O_2 in air in the empty cell were conducted by scanning the focused X-ray beam over an area of 5 μm × 5 μm of the graphene window. Figure S3 schematically shows the experimental step. The obvious difference in C 1s photoelectrons between in- and off-graphene window region suggested the presence of graphene membrane covering the through pore on Si_3N_4 (Figure 4b). In the image of O 1s mapping (Figure 4c), the non-homogeneous intensity distribution indicated the inhomogeneity of graphene membrane in terms of its thickness since O_2 molecules in air are homogeneously distributed in the cell (Figure S3). The doublet of O 1s photoemission intensity of molecular O_2 was observed at about 540 eV (Figure 4f), showing that gas phase O_2 of air was indeed filled to the Si_3N_4 membrane cell. In addition, the peak at ~534 eV is contributed from the oxygen-containing species of chemicals used in covering Si_3N_4 window with graphene membrane. In the survey XPS spectrum (Figure 4d), weak peaks assigned to Si 2p and Au 4f were also detected, attributable to Si_3N_4 and Au layers on the front surface of the window. The origin

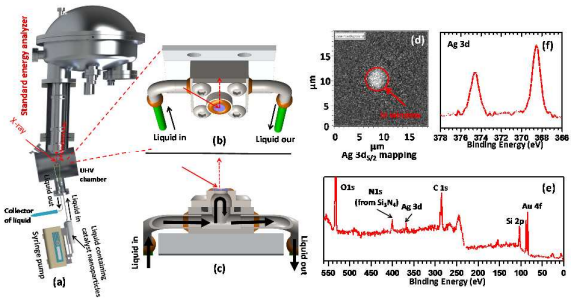

of Si 2p and Au 4f in Figure 4d can be found in Figure S4 and its note.

Figure 5. XPS studies of solution of Ag NPs flowing through window of Si_3N_4 membrane covered with a two-layer graphene membrane (flow rate: 0.5 mL·min^{-1}). The solution containing solvent (a mixture of tripropylene glycol methyl ether and phenol) and the Ag nanoparticles was pumped through a syringe pump. (a) The whole reactor system of flowing liquid. (b) and (c) External and internal structure of Si_3N_4 membrane cell with a window covered with graphene membrane. (d) Mapping of Ag 3d5/2 photoelectrons. (e) XPS survey of the window region (covered with graphene membrane) where solution of Ag NPs was flowing through the surface of graphene membrane with a slow rate of 0.5 mL·min^{-1}.

Successful study of surface of Ag NPs in flow liquid with XPS. After the blank experiment (Figure 4), the solution of Ag nanoparticles was pumped into the Si_3N_4 cell and flow through the surface of graphene membrane by using a syringe pump installed at inlet port in ambient condition (Figures 1a and S1). When the liquid containing Ag nanoparticles was flowing through the reaction system, the high contrast of Ag 3d contributed from Ag 3d photoelectrons at the in-window region was clearly observed in the mapping image of Ag 3d (Figure 5d) while the off-window region is dark in this image. It verified that these Ag 3d photoelectrons can definitely travel through the liquid layers between Ag nanoparticles and the two-layer graphene membrane and then penetrate the graphene membrane to reach the UHV environment of XPS chamber and then be collected by a standard energy analyzer. The presence of residual N1s, Si2p and Au4f in Figure 5c is believed to contribute from the Si_3N_4 and Au at the edge of the graphene window (Figure S4). The peak positon of Ag $3d_{5/2}$ at 367.5 eV in the XPS spectra (Figure 5f) suggests the surface Ag atoms of Ag nanoparticles were in metallic state. The successful observation of Ag 3d XPS peaks shows that metal nanoparticles dispersed in a flowing liquid can be characterized with XPS without using differentially pumped energy analyzer.

Conclusions

This work demonstrated the capability of studying surface of catalyst nanoparticles in a flowing liquid by using a high vacuum XPS with a standard energy analyzer instead of using differentially pumped energy analyzer. In this demonstration, a flowing reaction system was developed; its main parts include an inlet and an outlet to ensure the flow of the liquid with the assistance of a syringe pump, Si_3N_4 cell with an unique configuration to make sure the liquid flow through the surface of graphene window, and an electron-transparent graphene to separate the flowing liquid from the UHV environment of XPS analyzer chamber. This type of flowing liquid reaction cell has the capability of studying surface of catalyst nanoparticles in a flowing liquid at elevated temperatures, by which heterogeneous catalytic reactions performed at solid-liquid interface can be mimicked. It opens up opportunities for in-situ tracking the surface chemistry of a catalyst nanoparticles dispersed in flowing liquid during catalysis.

Acknowledgements

This work was supported by Chemical Sciences, Geosciences and Biosciences Division, Office of Basic Energy Sciences, Office of Science, U.S. Department of Energy, under Grant No. DE-SC0014561.

1. Ertl, G.; Knözinger, H.; Schüth, F.; Weitkamp, J.; Ertl, G.; Gerhard Ertl Ferdi Schuth, J. W. H. K.; Ertl, H.; Weitkamp, J. G.; Knozinger, *Handbook of Heterogeneous Catalysis*. 2nd ed.; Wiley-VCH: Weinheim, 2008; Vol. 2.

2. Somorjai Y. M, G. A.; Li; Somorjai, G. A.; Li, Y., *Introduction to Surface Chemistry and Catalysis*. 2 ed.; Wiley: Weinheim, 2010.

3. Tao, F.; Salmeron, M. *Science* **2011,** 331, (6014), 171-174.

4. Drummond, I. W. *Philos T R Soc A* **1996,** 354, (1719), 2667-2682.

5. Doron-Mor, H.; Hatzor, A.; Vaskevich, A.; van der Boom-Moav, T.; Shanzer, A.; Rubinstein, I.; Cohen, H. *Nature* **2000,** 406, (6794), 382-385.

6. Navarro, V.; van Spronsen, M. A.; Frenken, J. W. M. *Nat Chem* **2016,** 8, (10), 929-934.

7. Tundo, P.; Perosa, A. *Chem Soc Rev* **2007,** 36, (3), 532-550.

8. Climent, M. J.; Corma, A.; Iborra, S.; Sabater, M. J. *Acs Catal* **2014,** 4, (3), 870-891.

9. Dong, X.-Y.; Gao, Z.-W.; Yang, K.-F.; Zhang, W.-Q.; Xu, L.-W. *Catal. Sci. Technol.* **2015,** 5, (5), 2554-2574.

10. Farrauto, R. J., 3 From the internal combustion engine to the fuel cell: Moving towards the hydrogen economy. 2003; Vol. 145, pp 21-29.

11. Roy, S. C.; Varghese, O. K.; Paulose, M.; Grimes, C. a. *ACS Nano* **2010,** 4, (3), 1259-1278.

12. Kašpar, J.; Fornasiero, P.; Hickey, N. *Catalysis Today* **2003,** 77, (4), 419-449.

13. Favaro, M.; Jeong, B.; Ross, P. N.; Yano, J.; Hussain, Z.; Liu, Z.; Crumlin, E. J. *Nat Commun* **2016,** 7.

14. Trotochaud, L.; Head, A. R.; Karslioglu, O.; Kyhl, L.; Bluhm, H. *J Phys-Condens Mat* **2017,** 29, (5).

15. Brown, M. A.; Redondo, A. B.; Sterrer, M.; Winter, B.; Pacchioni, G.; Abbas, Z.; van Bokhoven, J. A. *Nano Lett* **2013,** 13, (11), 5403-5407.

16. Olivieri, G.; Brown, M. A. *Top Catal* **2016,** 59, (5-7), 621-627.

17. Brown, M. A.; Abbas, Z.; Kleibert, A.; Green, R. G.; Goel, A.; May, S.; Squires, T. M. *Phys Rev X* **2016,** 6, (1).

18. Soderstrom, J.; Ottosson, N.; Pokapanich, W.; Ohrwall, G.; Bjorneholm, O. *J Electron Spectrosc* **2011,** 184, (7), 375-378.

19. Liao, H. G.; Cui, L. K.; Whitelam, S.; Zheng, H. M. *Science* **2012,** 336, (6084), 1011-1014.

20. Zheng, H. M.; Smith, R. K.; Jun, Y. W.; Kisielowski, C.; Dahmen, U.; Alivisatos, A. P. *Science* **2009,** 324, (5932), 1309-1312.

21. Kolmakov, A.; Dikin, D. a.; Cote, L. J.; Huang, J.; Abyaneh, M. K.; Amati, M.; Gregoratti, L.; Günther, S.; Kiskinova, M. *Nature Nanotechnology* **2011,** 6, (10), 651-657.

22. Winter, B. *Nucl Instrum Meth A* **2009,** 601, (1-2), 139-150.

23. Weatherup, R. S.; Eren, B.; Hao, Y.; Bluhm, H.; Salmeron, M. B. *Journal of Physical Chemistry Letters* **2016,** 7, (9), 1622-1627.

24. Yulaev, A.; Guo, H.; Strelcov, E.; Chen, L.; Vlassiouk, I.; Kolmakov, A. *ACS Applied Materials & Interfaces* **2017,** 9, (31), 26492-26502.

25. Velasco-Vélez, J. J.; Pfeifer, V.; Hävecker, M.; Wang, R.; Centeno, A.; Zurutuza, A.; Algara-Siller, G.; Stotz, E.; Skorupska, K.; Teschner, D.; Kube, P.; Braeuninger-Weimer, P.; Hofmann, S.; Schlögl, R.; Knop-Gericke, A. *Review of Scientific Instruments* **2016,** 87, (5), 053121-053121.

26. Powell, C. J.; Jablonski, A., *NIST Electron Inelastic-Mean-Free-Path Database, Version 1.2, SRD 71*. National Institute of Standards and Technology, Gaithersburg, MD: 2010.

27. Tanuma, S.; Powell, C. J.; Penn, D. R. *Surf Interface Anal* **2011,** 43, (3), 689-713.

28. Son, J. H.; Song, Y. H.; Yu, H. K.; Lee, J. L. *Appl Phys Lett* **2009,** 95, (6).